

## **Supporting Information**

### **Carboxylative cyclization of atmospheric CO<sub>2</sub> with alkynol catalyzed by 1-methylhydantoin anion-functionalized ionic liquid via chelative interactions**

Yujun Guo, Tingting Chen and Yingjie Xu\*

Department of Chemistry, Shaoxing University, Shaoxing, Zhejiang Province, 312000, China.

Email: xuyj@usx.edu.cn

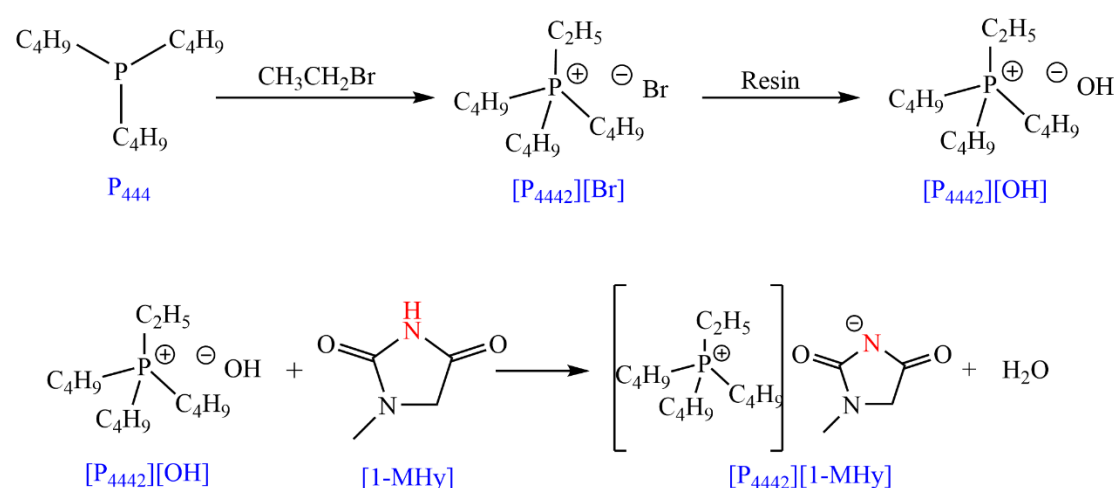
# 1. Experimental section: preparation of [P<sub>4442</sub>][1-MHy] and the reaction of MBY with CO<sub>2</sub> to prepare 4,4-dimethyl-5-methylidene-1,3-dioxolan-2-one

## 1.1 Materials

Tributylphosphine (P<sub>444</sub>, >98%), bromoethane (C<sub>2</sub>H<sub>5</sub>Br, >99%), sodium hydroxide (NaOH, >99%), ethanol (>99%) 2-methyl-3-butyn-2-ol (MBY, >98%), n-hexane (>99%) and a basic anion-exchange resin (Amberlite 717, AR) were purchased from Aladdin Reagent Co. Ltd., Shanghai, China. 1-Methylhydantoin (1-MHy, >99%) was purchased from Tokyo Chemical Industry Co., Ltd. CO<sub>2</sub> (>99.9%) and N<sub>2</sub> (>99.999%) were purchased from Hangzhou Jingong Gas Factory. All chemicals were used as received and obtained in highest purity grade possible.

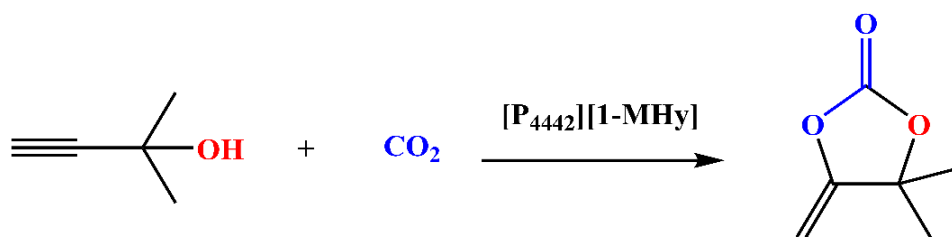
## 1.2 Synthesis and characterization of [P<sub>4442</sub>][1-MHy]

The synthesis process of [P<sub>4442</sub>][1-MHy] is similar to the literature.<sup>1</sup> Firstly, P<sub>444</sub> and C<sub>2</sub>H<sub>5</sub>Br were reacted under N<sub>2</sub> protection to obtain the tributylethylphosphonium bromide ([P<sub>4442</sub>][Br]). Secondly, [P<sub>4442</sub>][Br] was passed through the basic anion-exchange resin activated by NaOH to obtain the tributylethylphosphonium hydroxide ([P<sub>4442</sub>][OH]) ethanol solution. Finally, [P<sub>4442</sub>][1-MHy] was synthesized via the neutralization by [P<sub>4442</sub>][OH] with 1-MHy in a 1:1 molar ratio at 50 °C for 24 h. The specific reaction equations are shown in Scheme S1. Ethanol and water were removed from the [P<sub>4442</sub>][1-MHy] under vacuum at 70 °C. Trace amount of water was removed from [P<sub>4442</sub>][1-MHy] by a freeze dryer. The water content in [P<sub>4442</sub>][1-MHy] determined by Karl Fisher titration (Mettler Toledo C20S) was 1001.6 ppm. The structure of [P<sub>4442</sub>][1-MHy] was characterized by <sup>1</sup>H NMR and <sup>13</sup>C NMR spectra with Bruker AVANCE III spectrometer (Fig. S2).



**Scheme S1** Synthesis of [P<sub>4442</sub>][1-MHy]

## 1.3 The [P<sub>4442</sub>][1-MHy]-catalyzed reaction of MBY and CO<sub>2</sub> to 4,4-dimethyl-5-methylene-1,3-dioxolan-2-one and reusability of [P<sub>4442</sub>][1-MHy]



**Scheme S2** [P<sub>4442</sub>][1-MHy]-catalyzed reaction of CO<sub>2</sub> and MBY to 4,4-dimethyl-5-methylene-1,3-dioxolan-2-one

**The typical reaction process at 0.1 MPa CO<sub>2</sub> is as follows:** MBY (12 mmol) and [P<sub>4442</sub>][1-MHy] (1.2 mmol) were added to a round-bottomed flask fitted with a condenser, and CO<sub>2</sub> was slowly and continuously drummed into the reaction system, which was stirred at 60 °C for 15 h. Other atmospheric pressure reaction procedures were similar to those described above. The reaction equation was shown in Scheme S2. The yield of product was determined by <sup>1</sup>H NMR spectroscopy using [P<sub>4442</sub>][1-MHy] as an internal standard. The effect of the temperature on the reaction at 0.1 MPa CO<sub>2</sub> for 15 h was shown in Fig. S3.

**The typical reaction process at CO<sub>2</sub> pressure higher than 0.1 MPa:** MBY (12 mmol) and [P<sub>4442</sub>][1-MHy] (1.2 mmol) were added to a miniature reactor containing a magneton (YZQR-100), and CO<sub>2</sub> was injected into the reactor through a stainless steel vent tube to ensure that the CO<sub>2</sub> pressure was 1.0 MPa, and stirred at 60 °C for 6 h. The reaction at other pressures were similar to those described above. The effect of the amount of [P<sub>4442</sub>][1-MHy] on the reaction at 1.0 MPa CO<sub>2</sub> and 60 °C for 6 h was shown in Fig. S4.

**The separation and purification of the product and the recovery of [P<sub>4442</sub>][1-MHy]:** after finishing the reaction, n-hexane was added to the reaction system in batches (4×12 mL) and stirred, and the system was stratified at rest, with n-hexane containing the product in the upper layer, and [P<sub>4442</sub>][1-MHy] in the lower layer. The upper solution was collected, the pure product was obtained by evaporation to remove n-hexane, and the isolated product was freeze-dried and the structure was characterized by NMR spectra (Fig. S5), and finally the isolated yield was calculated. The melting and boiling points of the product were determined by DSC (Fig. S6). In addition, after vacuum drying the lower layer [P<sub>4442</sub>][1-MHy] to remove trace amounts of n-hexane, it was placed in a freeze dryer to remove trace amounts of water, and then the recovered [P<sub>4442</sub>][1-MHy] was used for the next catalytic reaction (Fig. S7). Finally, the structure of the recycled [P<sub>4442</sub>][1-MHy] after five cycles was characterized by <sup>1</sup>H NMR spectra (Fig. S8).

#### 1.4 Measurement of <sup>1</sup>H NMR Spectra of [P<sub>4442</sub>][1-MHy] + MBY mixtures

The binary mixtures of [P<sub>4442</sub>][1-MHy] + MBY were prepared by mass using a Mettler Toledo AL204 analytical balance with a stated precision of ±0.0001 g. The concentration-dependent <sup>1</sup>H NMR chemical shifts of the binary mixtures were measured at 25 °C with the Bruker AVANCE

III 400MHz using the internal reference method, which was described in previous works.<sup>2,3</sup> The specific measurement process was as follows: to avoid the influence of deuterated reagents on the  $^1\text{H}$  NMR chemical shifts of the sample, the deuterium oxide ( $\text{D}_2\text{O}$ ) was sealed in a 2 mm capillary tube, which was placed at the center of a 5 mm sample tube filled with the sample and chemical shift reference of tetramethylsilane (TMS). It is necessary to keep the inner capillary tube parallel to the exterior sample tube. The concentration-dependent  $^1\text{H}$  NMR spectra of  $[\text{P}_{4442}][1\text{-MHy}]^- + \text{MBY}$  mixtures are plotted in Fig. S9. As shown in Fig. S9, the peak at about 4.5 ppm of pure MBY can be assigned to  $-\text{OH}$ , and its chemical shift ( $\delta$ ) gradually shifts to the lower field with increasing molar fraction of IL ( $x_{\text{IL}}$ ), accompanied by a change from a sharp peak to a broad peak, suggesting the formation of a strong hydrogen bond interaction (H-bond) with  $[1\text{-MHy}]^-$ . The peak at 2.5 ppm of pure MBY is  $\text{C}\equiv\text{C-H}$  and its  $\delta$  remains essentially unchanged in the range of  $0 < x_{\text{IL}} < 0.2$  and increases slightly when  $x_{\text{IL}} > 0.2$ , indicating that the H-bond of  $[1\text{-MHy}]^-$  with  $\text{C}\equiv\text{C-H}$  is much weaker than that of  $[1\text{-MHy}]^-$  with  $-\text{OH}$ .  $\delta$  of the methyl ( $-\text{CH}_3$ ) of MBY remains essentially constant with increasing  $x_{\text{IL}}$ , indicating that the weak physical interaction is dominant between  $[1\text{-MHy}]^-$  and  $-\text{CH}_3$ .

## 2. Computation method

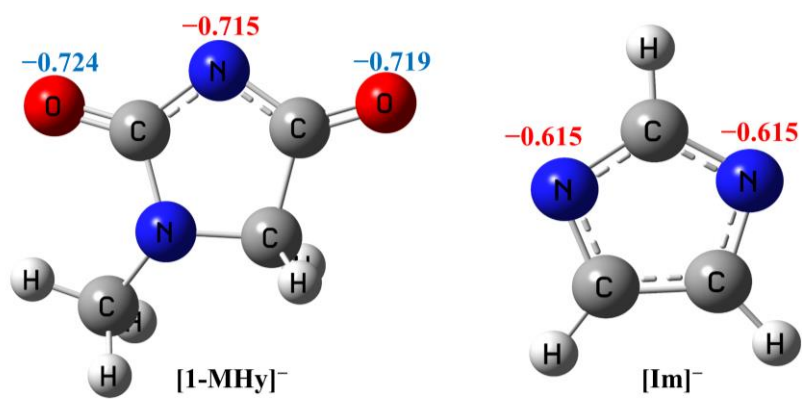
The geometry optimizations and frequency calculations of MBY and  $[1\text{-MHy}]^-$  were obtained by DFT calculations at the wB97XD/6-31++G(d, p) basis set with the Gaussian 09 D.01 program.<sup>4</sup> The optimized geometries of MBY,  $[1\text{-MHy}]^-$ ,  $[\text{Im}]^-$ , and H-bond complexes of the anion with  $-\text{OH}$  or  $\text{C}\equiv\text{C-H}$  were recognized as local minima with no imaginary frequency, then the bond length was obtained. The interaction energy ( $\Delta E$ ) of the H-bond was calculated as the difference between the energy of the complex and the energy sum of the optimized monomers. The NBO charges of MBY,  $[1\text{-MHy}]^-$ ,  $[\text{Im}]^-$ , and H-bond complexes were obtained using natural bond orbital (NBO) analysis. The energies for the conversion of TS2 into product processes such  $\Delta G$  and  $\Delta H$  were calculated at the wB97XD/6-31++G(d, p) basis set with the Gaussian 09 D.01 program. The optimized geometries and NBO charges of  $[1\text{-MHy}]^-$  and  $[\text{Im}]^-$  anions were shown in Fig. S1.

## 3. In situ FT-IR spectra experiment

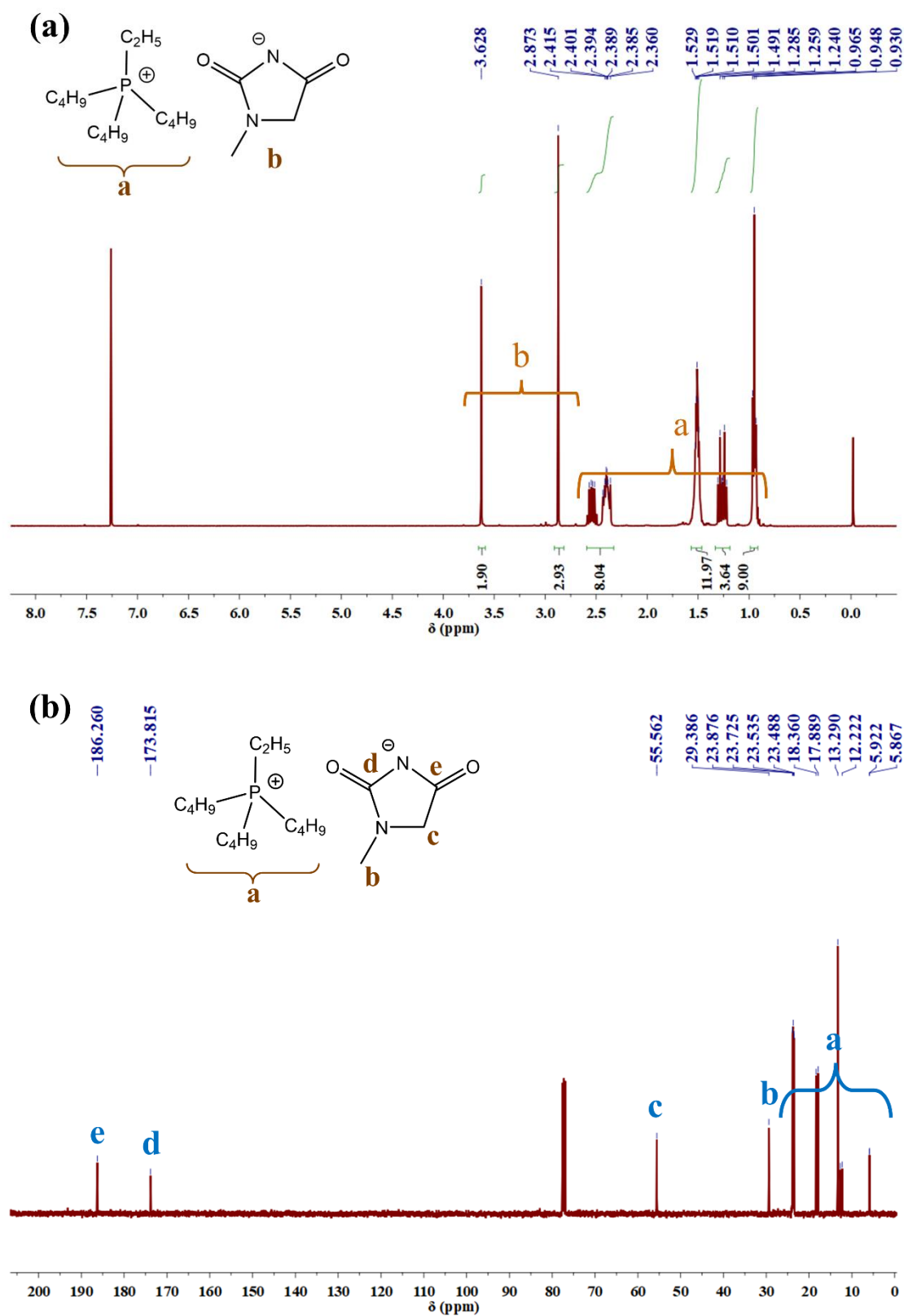
To determine the attribution of the functional group peaks of pure MBY,  $[\text{P}_{4442}][1\text{-MHy}]$  and the product, FT-IR spectra were recorded on a Nicolet 6700 Fourier transform infrared spectrometer equipped with a DTGS detector and ATR accessory. ATR-IR spectrum was recorded with a resolution of  $2\text{ cm}^{-1}$  and 16 parallel scans, and the wavenumber was in the range from 4000 to  $600\text{ cm}^{-1}$ .<sup>5,6</sup> The FT-IR spectra of pure MBY,  $[\text{P}_{4442}][1\text{-MHy}]$  and the product were shown in Fig. S17.

*In situ* FT-IR spectra were recorded using a ReactIR 702L (Mettler Toledo) equipped with a 9.5 mm diameter DiComp ATR probe with a 1.5-meter fiber.<sup>7,8</sup> *In situ* FT-IR spectra were collected at

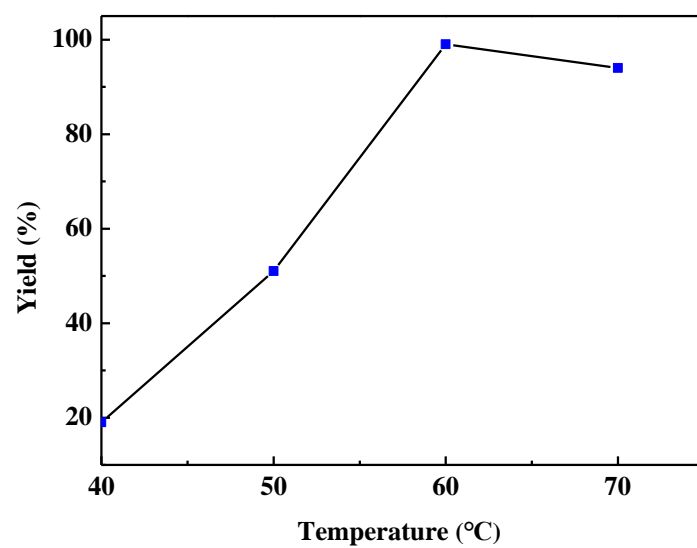
4 cm<sup>-1</sup> resolutions and 64 scans with a range of 3000–800 cm<sup>-1</sup>. Diamond transmits IR over most of this region apart from absorption regions of 2200–1900 cm<sup>-1</sup> and below 650 cm<sup>-1</sup>.<sup>9</sup> This does not affect probe performance as the fingerprint region (1850–650 cm<sup>-1</sup>) was used to monitor catalytic conversion of CO<sub>2</sub> and MBY to 4,4-dimethyl-5-methylene-1,3-dioxolan-2-one by [P<sub>4442</sub>][1-MHy]. The ATR probe equipped with RTO sensor was submerged in the reaction vessel and spectra and temperature data collected throughout the reaction (the molar ratio of [P<sub>4442</sub>][1-MHy] to MBY as 1:10, 80 °C with stirring and bubbling CO<sub>2</sub>). It should be noted that the background spectrum was collected at actual reaction conditions at the same data collection parameters and the same optical bench as subsequent reaction spectra, and was subtracted from the experimental data.



**Fig. S1** The optimized geometries and NBO charges of [1-MHy]<sup>-</sup> and [Im]<sup>-</sup> anions.

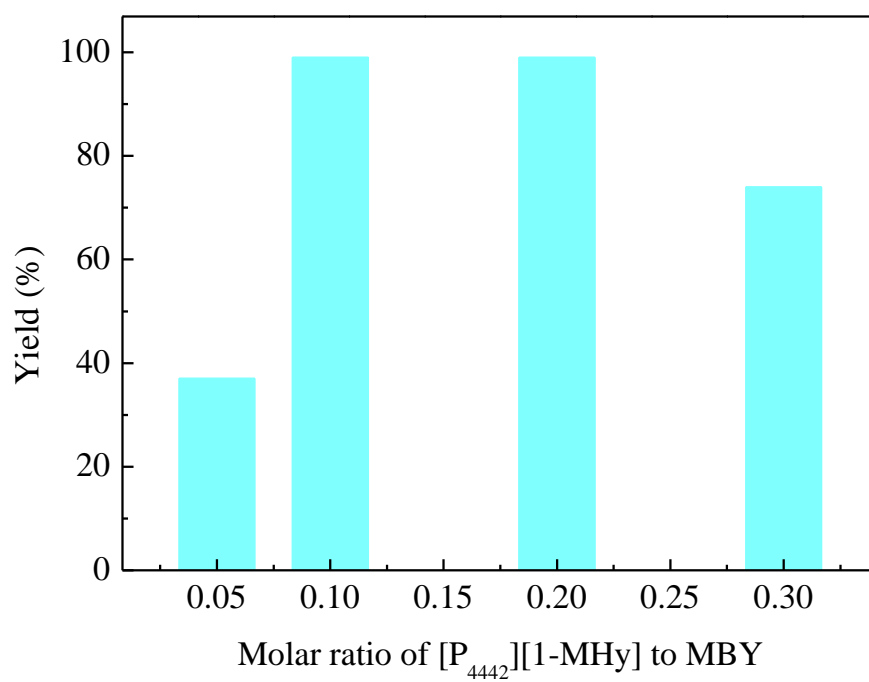


**Fig. S2** NMR spectra of  $[P_{442}][1\text{-MHy}]$  (chloroform- $d$ ). (a)  $^1\text{H}$  NMR chemical shift of cation,  $\delta/\text{ppm}$ : 0.93-0.97 (m, 9H,  $\text{CH}_3$ ), 1.24-1.29 (m, 3H,  $\text{CH}_3$ ), 1.49-1.53 (m, 12H,  $\text{CH}_2$ ), 2.36-2.42 (m, 8H,  $\text{PCH}_2$ ); anion,  $\delta/\text{ppm}$ : 2.87 (s, 3H,  $\text{CH}_3$ ), 3.63 (s, 2H,  $\text{CH}_2$ ). (b)  $^{13}\text{C}$  NMR chemical shift of cation,  $\delta/\text{ppm}$ : 5.87-23.9 ( $\text{CH}_3$ ,  $\text{CH}_2$ ); anion, 29.4 ( $\text{CH}_3$ ), 55.6 ( $\text{CH}_2$ ), 173.9 and 186.3 ( $\text{C}=\text{O}$ s).

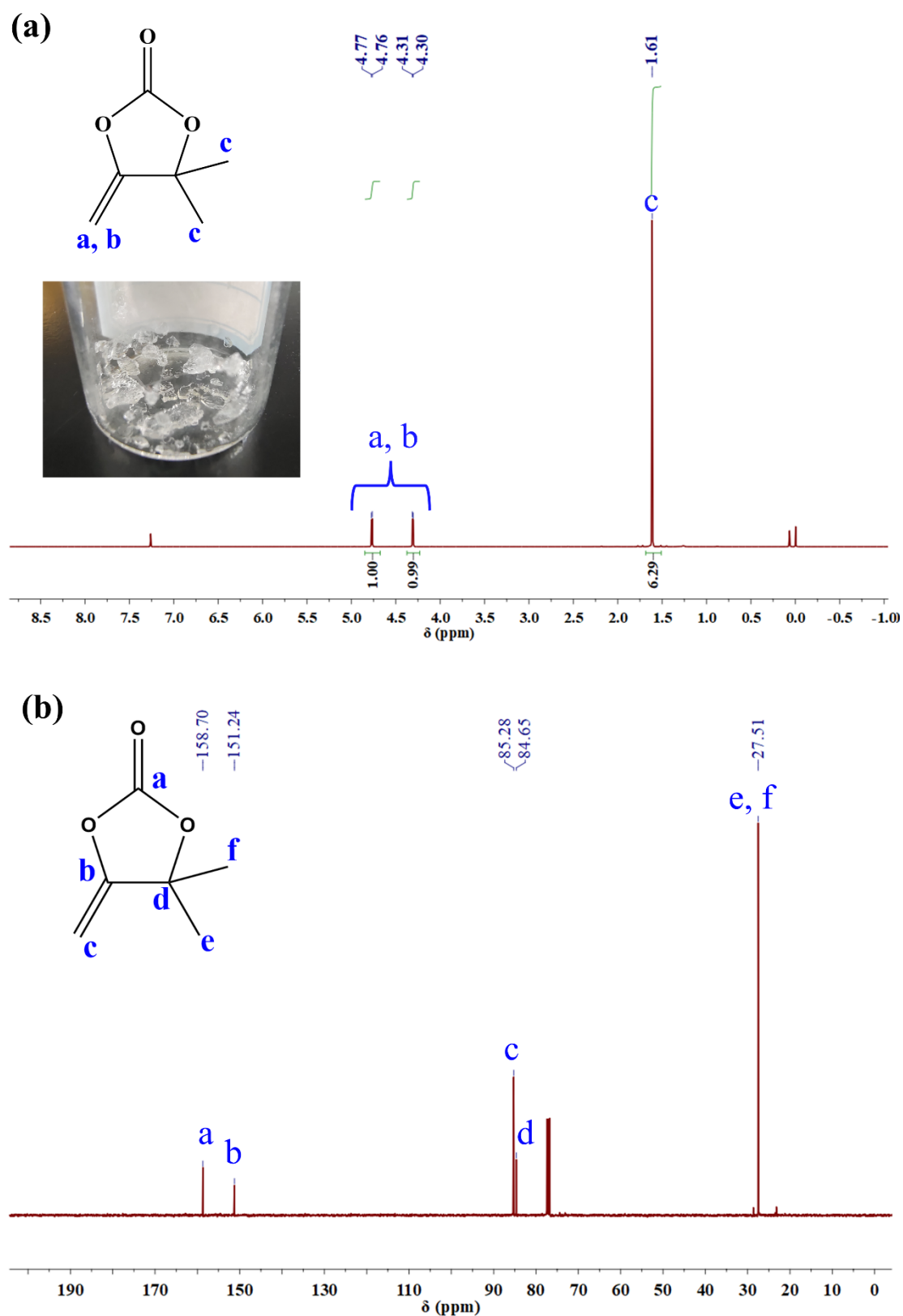


**Fig. S3** The effect of the temperature on the reaction at 0.1 MPa CO<sub>2</sub> for 15 h.

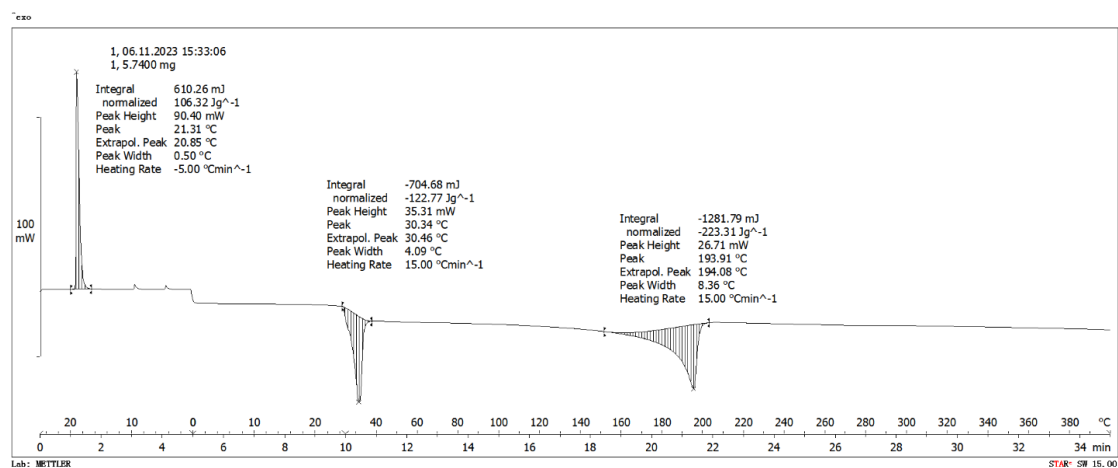




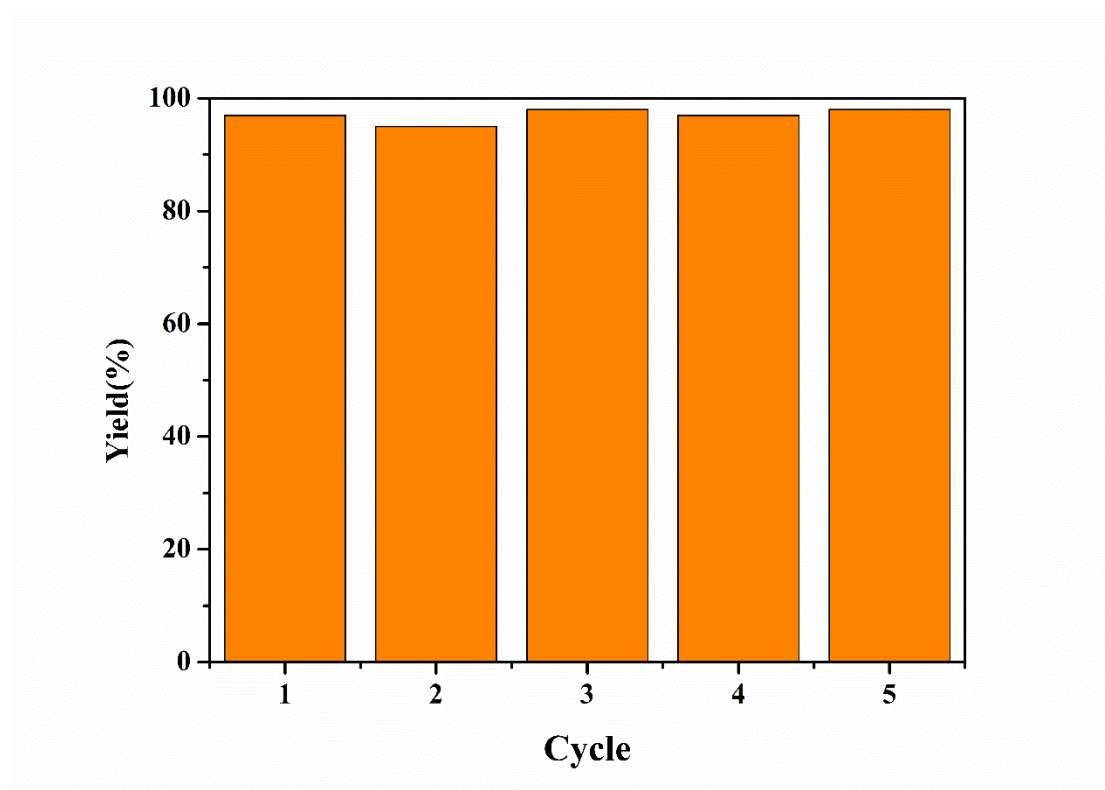
**Fig. S4** The effect of the amount of  $[P_{442}][1-MHy]$  on the reaction of  $CO_2$  with MBY at 60 °C and 1.0 MPa for 6 h.



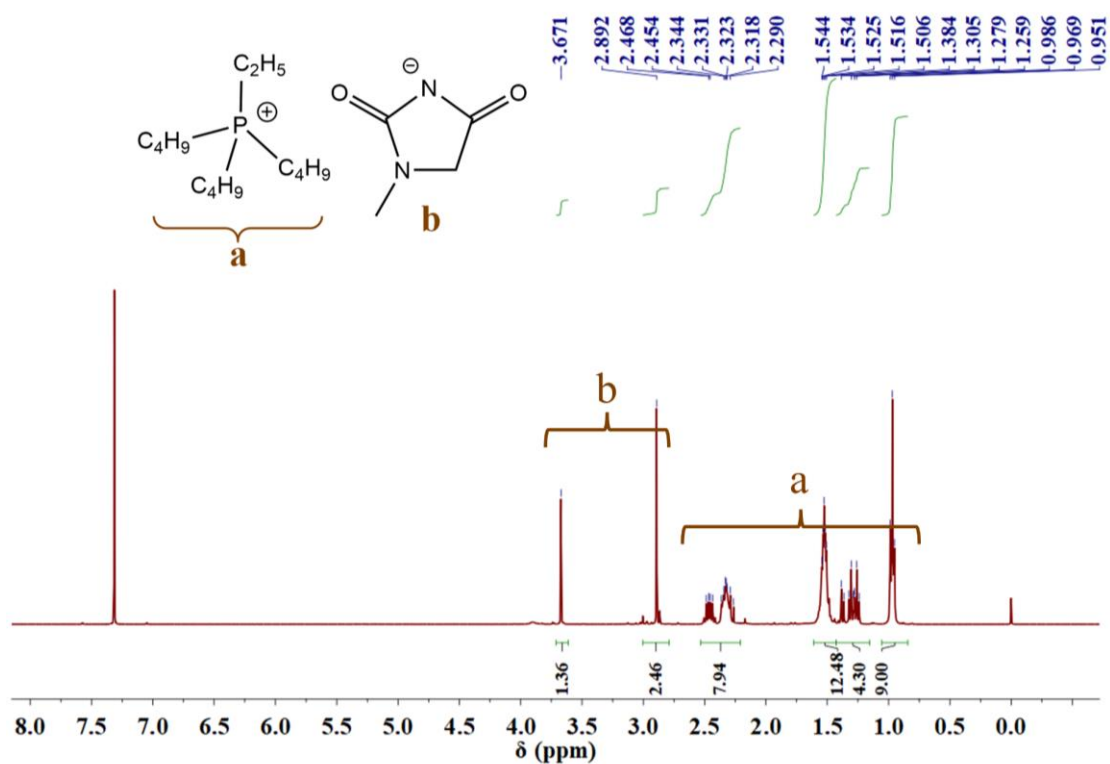
**Fig. S5** The state of the isolated 4,4-dimethyl-5-methylene-1,3-dioxolan-2-one at room temperature and NMR spectra (chloroform-*d*). (a)  $^1\text{H}$  NMR chemical shift,  $\delta/\text{ppm}$ : 1.61 (s, 6H,  $\text{CH}_3$ ), 4.30-4.77 (s, H, CH); (b)  $^{13}\text{C}$  NMR chemical shift,  $\delta/\text{ppm}$ : 27.51 ( $\text{CH}_3$ ), 84.65 (C-O), 85.28 ( $\text{O}-\text{C}=\text{C}^*\text{H}_2$ ), 151.24 ( $\text{O}-\text{C}^*=\text{CH}_2$ ), 158.70 ( $\text{C}=\text{O}$ ).



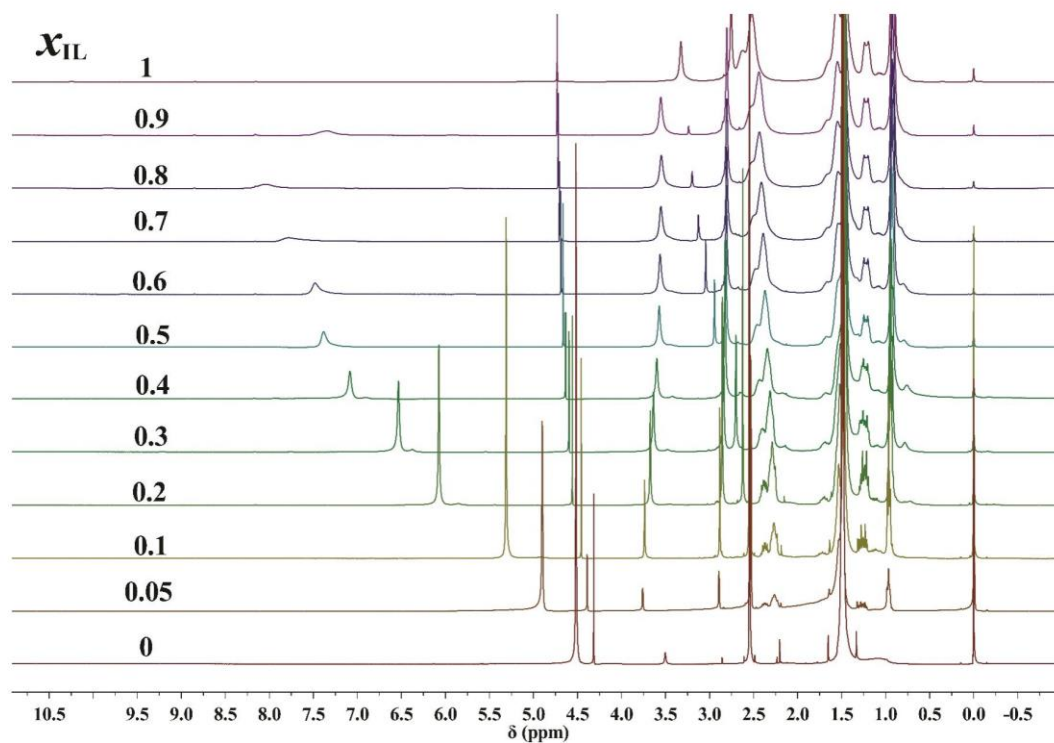
**Fig. S6** DSC curve of 4,4-dimethyl-5-methylene-1,3-dioxolan-2-one.



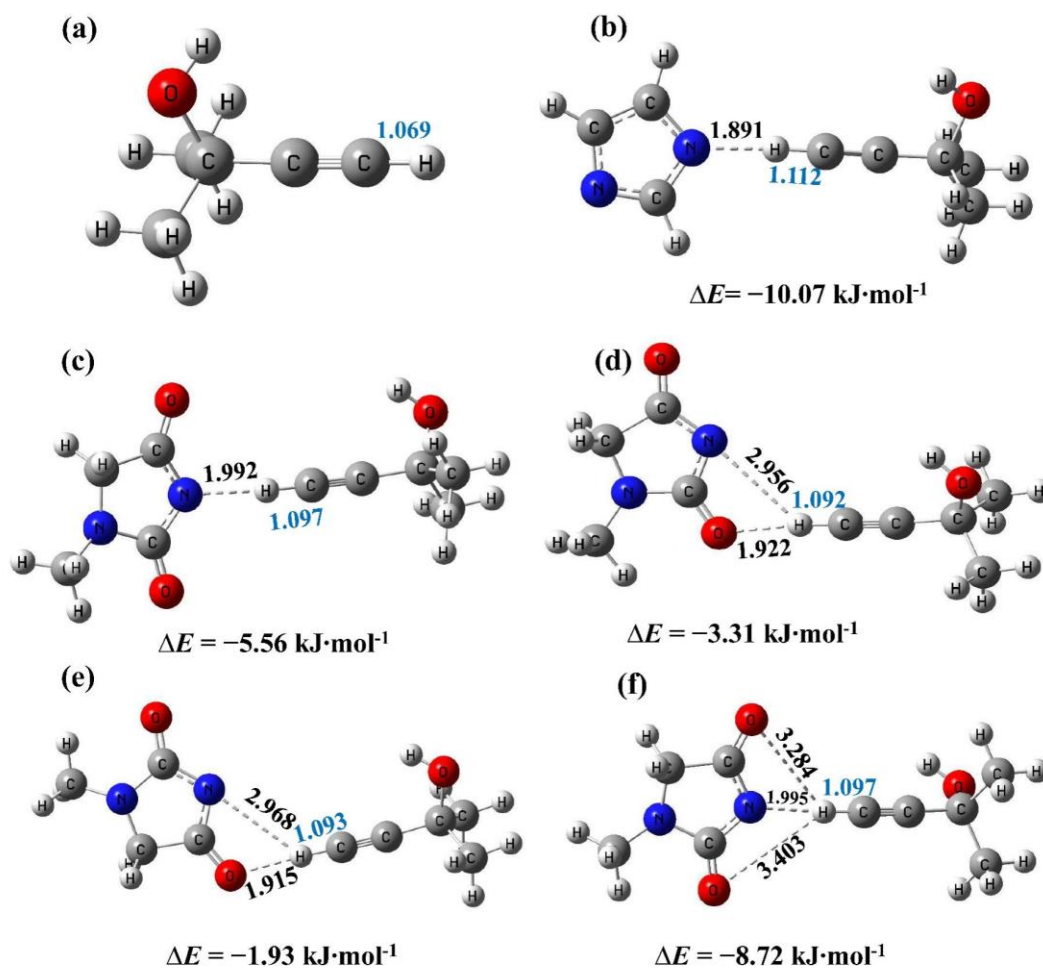
**Fig. S7** Reusability of [P<sub>4442</sub>][1-MHy] to catalyze the reaction of MBY and CO<sub>2</sub> for five successive cycles. [P<sub>4442</sub>][1-MHy]: MBY = 1:10, 1.0 MPa CO<sub>2</sub>, 60 °C for 6 h. The yields were determined by <sup>1</sup>H NMR spectra using [P<sub>4442</sub>][1-MHy] as an internal standard.



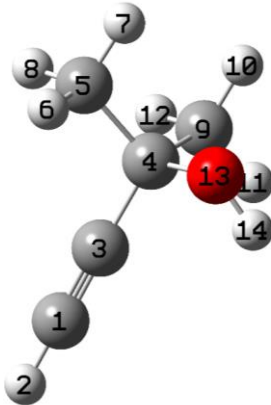
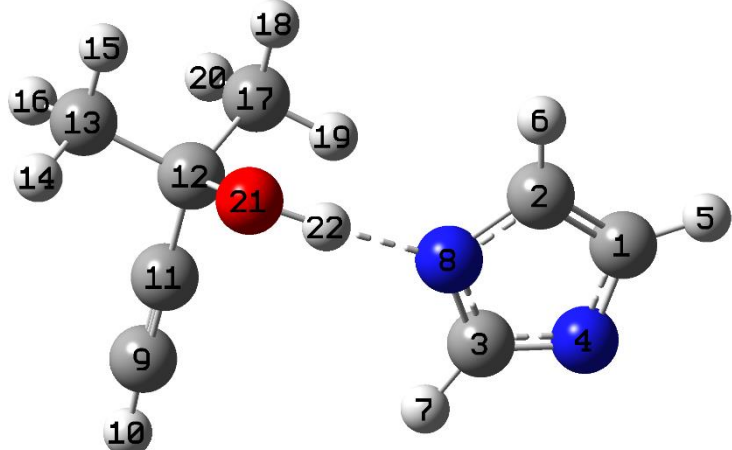
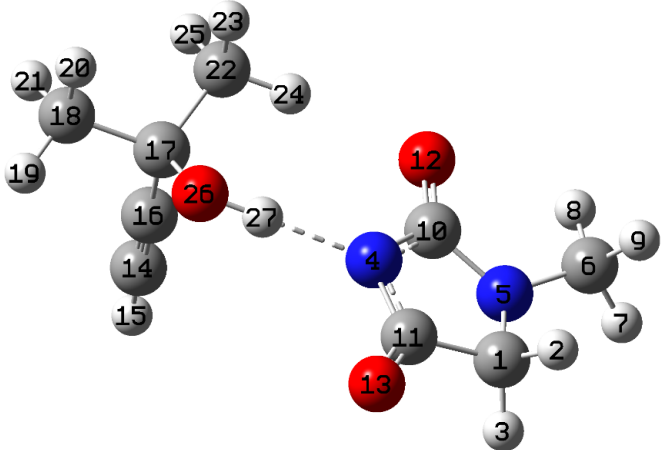
**Fig. S8**  $^1\text{H}$  NMR spectra (chloroform-*d*) of recovered [P<sub>4442</sub>][1-MHy] after the fifth cycle. Cation,  $\delta/\text{ppm}$ : 0.95-0.99 (m, 9H, CH<sub>3</sub>), 1.26-1.38 (m, 3H, CH<sub>3</sub>), 1.52-1.54 (m, 12H, CH<sub>2</sub>), 2.29-2.47 (m, 8H, CH<sub>2</sub>); anion,  $\delta/\text{ppm}$ : 2.89 (s, 3H, CH<sub>3</sub>), 3.67 (s, 2H, CH<sub>2</sub>).

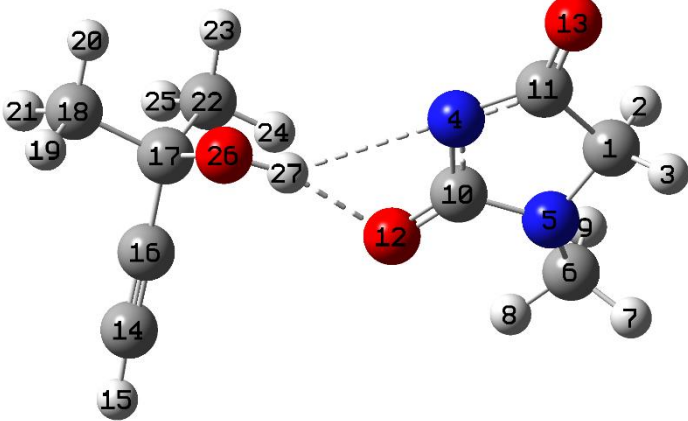
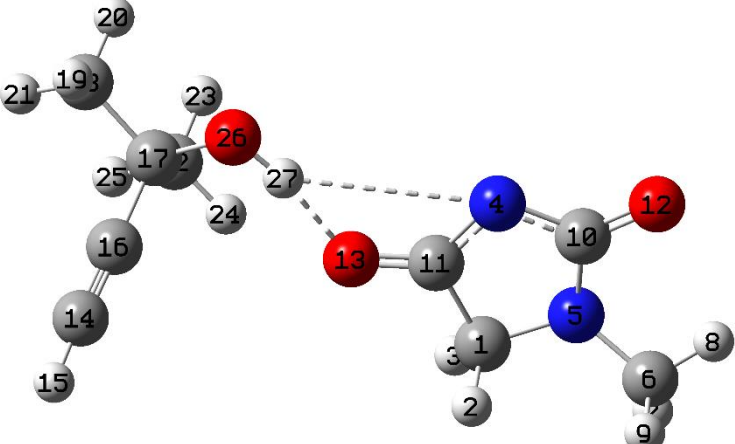


**Fig. S9**  $^1\text{H}$  NMR spectra of [P<sub>4442</sub>][1-MHy] + MBY mixture.



**Fig. S10** Optimized geometries, bond length ( $\text{\AA}$ ), and interaction energy ( $\Delta E$ ) of H-bonds between anion and  $\text{C}\equiv\text{C}-\text{H}$  of MBY. (a) MBY. The single H-bond: (b),  $[\text{IM}]^-$  and  $\text{C}\equiv\text{C}-\text{H}$ ; (c),  $[\text{1-MHy}]^-$  and  $\text{C}\equiv\text{C}-\text{H}$ . Chelative interactions between  $[\text{1-MHy}]^-$  and  $\text{C}\equiv\text{C}-\text{H}$ : (d), (e), (f).

Figs. S11-S16 The optimized geometries and NBO charges of the interactions between the anion and -OH of MBY. (C atom is gray, N atom is blue, O atom is red, H atom is white)		NBO charges	
<b>Fig. S11</b> MBY.		1	C -0.22707
		2	H 0.24611
		3	C -0.05872
		4	C 0.16068
		5	C -0.63573
		6	H 0.24311
		7	H 0.23699
		8	H 0.23095
		9	C -0.64431
		10	H 0.23718
		11	H 0.22918
		12	H 0.23277
		13	O -0.74279
		14	H 0.49165
<b>Fig. S12</b> Single H-bond of [IM] <sup>-</sup> with -OH of MBY.		1	C -0.17724
		2	C -0.17051
		3	C 0.10905
		4	N -0.59229
		5	H 0.19832
		6	H 0.20379
		7	H 0.19314
		8	N -0.64978
		9	C -0.30707
		10	H 0.23751
		11	C -0.00108
		12	C 0.18412
		13	C -0.65689
		14	H 0.23744
		15	H 0.23266
		16	H 0.21908
		17	C -0.67706
		18	H 0.22924
		19	H 0.26701
		20	H 0.21583
		21	O -0.82080
		22	H 0.52553
<b>Fig. S13</b> Single H-bond of [1-MHy] <sup>-</sup> with -OH of MBY.		1	C -0.33103
		2	H 0.21957
		3	H 0.22867
		4	N -0.75143
		5	N -0.56927
		6	C -0.44951
		7	H 0.20551
		8	H 0.25407
		9	H 0.19406
		10	C 0.82243
		11	C 0.66673
		12	O -0.71522
		13	O -0.68859
		14	C -0.30237
		15	H 0.23596
		16	C 0.00198
		17	C 0.18308

	18 C -0.65603 19 H 0.23797 20 H 0.23246 21 H 0.21968 22 C -0.68522 23 H 0.22452 24 H 0.28339 25 H 0.21297 26 O -0.80563 27 H 0.53124
<p><b>Fig. S14</b> Chelative interactions of [1-MHy]<sup>-</sup> with -OH of MBY.</p> 	1 C -0.3343 2 H 0.21991 3 H 0.22829 4 N -0.71498 5 N -0.5662 6 C -0.45033 7 H 0.20572 8 H 0.25628 9 H 0.19488 10 C 0.81544 11 C 0.65403 12 O -0.75207 13 O -0.69741 14 C -0.31625 15 H 0.23601 16 C 0.00689 17 C 0.18081 18 C -0.65923 19 H 0.23561 20 H 0.24054 21 H 0.22042 22 C -0.68126 23 H 0.2701 24 H 0.25079 25 H 0.21712 26 O -0.79824 27 H 0.53743
<p><b>Fig. S15</b> Chelative interactions of [1-MHy]<sup>-</sup> with -OH of MBY.</p> 	1 C -0.32663 2 H 0.22114 3 H 0.22731 4 N -0.69146 5 N -0.57507 6 C -0.45048 7 H 0.20426 8 H 0.25352 9 H 0.19370 10 C 0.80935 11 C 0.65865 12 O -0.70443 13 O -0.75729 14 C -0.30237 15 H 0.23715 16 C 0.00077 17 C 0.18437 18 C -0.65795 19 H 0.23987 20 H 0.23580

	21	H	0.22101
	22	C	-0.67936
	23	H	0.23322
	24	H	0.26835
	25	H	0.21707
	26	O	-0.79813
	27	H	0.53764
<b>Fig. S16</b> Chelative interactions of [1-MHy] <sup>-</sup> with -OH of MBY.			
	1	C	-0.32746
	2	H	0.22148
	3	H	0.22690
	4	N	-0.75062
	5	N	-0.57265
	6	C	-0.44916
	7	H	0.20389
	8	H	0.25417
	9	H	0.19452
	10	C	0.82292
	11	C	0.66759
	12	O	-0.69948
	13	O	-0.70589
	14	C	-0.30284
	15	H	0.23486
	16	C	0.00449
	17	C	0.18189
	18	C	-0.65607
	19	H	0.2385
	20	H	0.23276
	21	H	0.21964
	22	C	-0.68416
	23	H	0.22464
	24	H	0.28136
	25	H	0.21289
	26	O	-0.80511
	27	H	0.53090



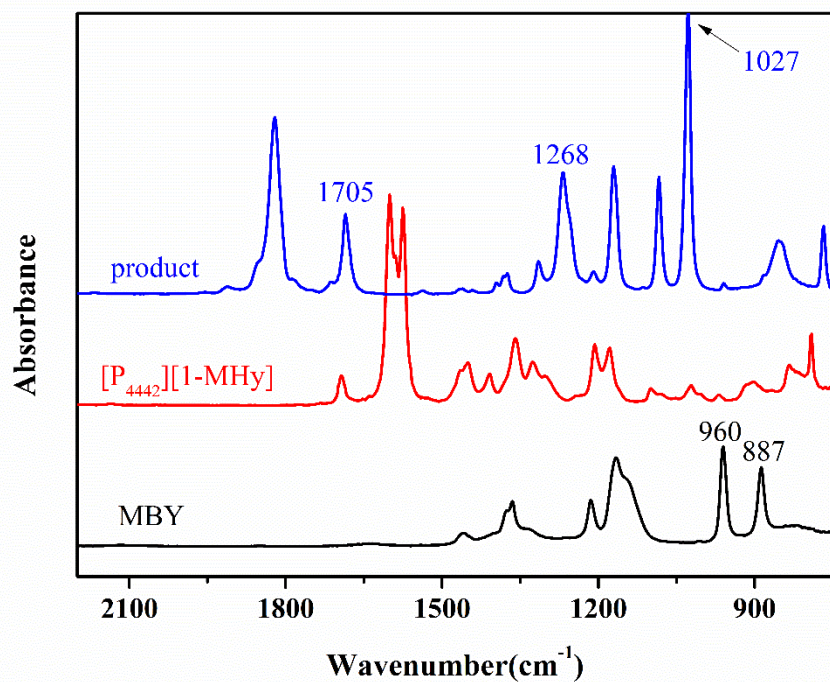


**Fig. S17** FT-IR spectra of pure MBY, [P<sub>442</sub>][1-MHy], and the product.

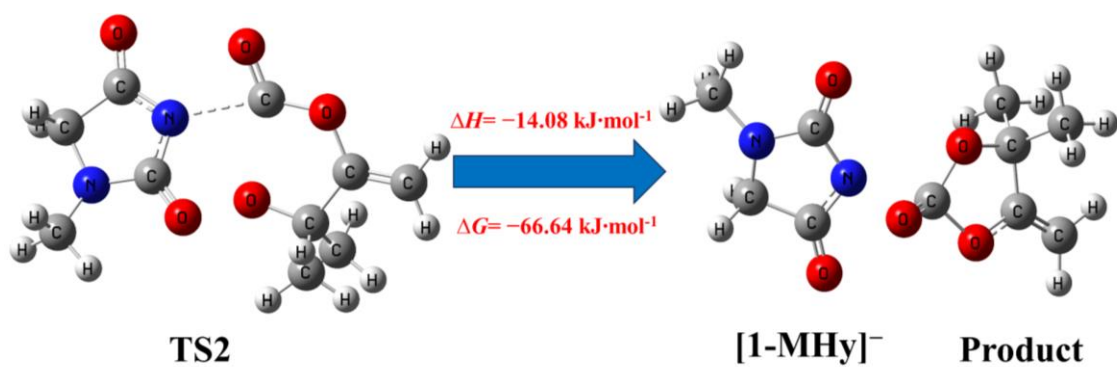


**Fig. S18** Optimized structure for TS2 and the energy of its conversion to product at wB97XD/6-31++G(d, p) basis set (C atom is gray, N atom is blue, O atom is red, H atom is white).

## References

1. C. Wang, X. Luo, H. Luo, D. E. Jiang, H. Li and S. Dai, *Angew. Chem. Int. Ed.*, 2011, **50**, 4918-4922.
2. J. Liu, X. Tang, H. Lu and Y. Xu, *ACS Sustainable Chem. Eng.*, 2021, **9**, 5050-5060.
3. Y. Xu, Y. Gao, L. Zhang, J. Yao, C. Wang and H. Li, *Sci. China Chem.*, 2010, **53**, 1561-1565.
4. M. J. Frisch, G. W. Trucks, H. B. Schlegel, G. E. Scuseria, M. A. Robb, J. R. Cheeseman, G. Scalmani, V. Barone, B. Mennucci, G. A. Petersson, H. Nakatsuji, M. Caricato, X. Li, H. P. Hratchian, A. F. Izmaylov, J. Bloino, G. Zheng, J. L. Sonnenberg, M. Hada, M. Ehara, K. Toyota, R. Fukuda, J. Hasegawa, M. Ishida, T. Nakajima, Y. Honda, O. Kitao, H. Nakai, T. Vreven, J. A. Montgomery, Jr., J. E. Peralta, F. Ogliaro, M. Bearpark, J. J. Heyd, E. Brothers, K. N. Kudin, V. N. Staroverov, R. Kobayashi, J. Normand, K. Raghavachari, A. Rendell, J. C. Burant, S. S. Iyengar, J. Tomasi, M. Cossi, N. Rega, N. J. Millam, M. Klene, J. E. Knox, J. B. Cross, V. Bakken, C. Adamo, J. Jaramillo, R. Gomperts, R. E. Stratmann, O. Yazyev, A. J. Austin, R. Cammi, C. Pomelli, J. W. Ochterski, R. L. Martin, K. Morokuma, V. G. Zakrzewski, G. A. Voth, P. Salvador, J. J. Dannenberg, S. Dapprich, A. D. Daniels, Ö. Farkas, J. B. Foresman, J. V. Ortiz, J. Cioslowski, D. J. Fox, *Gaussian 09*, R. D. 01, Gaussian, Inc., Wallingford CT, 2009.
5. Y. Xu, T. Li, C. Peng and H. Liu, *Ind. Eng. Chem. Res.*, 2015, **54**, 9038-9045.
6. J. Liu, X. Tang, H. Lu and Y. Xu, *ACS Sustainable Chem. Eng.*, 2021, **9**, 5050-5060.
7. L. Wang, F. Zhang, Y. Liu, S. Du and J. Leng, *ACS Appl. Mater. Interfaces*, 2021, **13**, 18110-18119.
8. A. Castro-Ruiz, L. Grefe, E. Mejía and S. G. Suman, *Dalton T.*, 2023, **52**, 4186-4199.
9. A. Pintar, R. Malacea, C. Pinel and M. Besson, *Vib. Spectrosc.*, 2007, **45**, 18-26.